Eur Respir J 2003; 22: 20–27
DOI: 10.1183/09031936.03.00108603
Printed in UK – all rights reserved

European Respiratory Journal
ISSN 0903-1936

Therapeutic potential of a new phosphodiesterase inhibitor in acute lung injury

P.R.M. Rocco*, D.P. Momesso*, R.C. Figueira*, H.C. Ferreira*, R.A. Cadete*, A. Légora-Machado#, V.L.G. Koatz#, L.M. Lima¶, E.J. Barreiro¶, W.A. Zin*

Therapeutic potential of a new phosphodiesterase inhibitor in acute lung injury. P.R.M. Rocco, D.P. Momesso, R.C. Figueira, H.C. Ferreira, R.A. Cadete, A. Légora-Machado, V.L.G. Koatz, L.M. Lima, E.J. Barreiro, W.A. Zin. ©ERS Journals Ltd 2003.

ABSTRACT: The effects of LASSBio596, a phosphodiesterase type-4 and -5 inhibitor, were tested in *Escherichia coli* lipopolysaccharide (LPS)-induced acute lung injury.

Twenty-four BALB/c mice were randomly divided into four groups. In the control group, saline (0.05 mL) was injected intratracheally (*i.t.*). The LPS group received LPS (10 μg *i.t.*, 0.05 mL). In the LASSBio596 groups, LASSBio596 (10 mg·kg^{-1}, 0.2 mL) was injected intraperitoneally 1 h before or 6 h after LPS administration. After 24 h, *in vivo* (lung resistive and viscoelastic pressures, and static and dynamic elastances) and *in vitro* (tissue resistance, elastance and hysteresivity) pulmonary mechanics, lung morphometry and collagenous fibre content were computed. Neutrophils and tumour necrosis factor (TNF)-α levels were evaluated in the bronchoalveolar lavage fluid.

LASSBio596 prevented the changes in lung mechanics, and inhibited neutrophilic recruitment, TNF-α release, bronchoconstriction, alveolar collapse and the increment of collagen fibre content induced by LPS, independently of the moment of injection.

In conclusion, LASSBio596 modulated the lung inflammatory process and had the potential to block fibroproliferation. Thus, agents that inhibit phosphodiesterase 4 and 5 simultaneously may be a useful adjunct therapy for acute lung injury.
Eur Respir J 2003; 22: 20–27.

*Laboratory of Respiration Physiology, Carlos Chagas Filho Biophysics Institute, #Dept of Medical Biochemistry and ¶Laboratório de Avaliação e Síntese de Substâncias Bioativas (LASSBio), Federal University of Rio de Janeiro, Rio de Janeiro, Brazil.

Correspondence: W.A. Zin, Universidade Federal do Rio de Janeiro, Instituto de Biofísica Carlos Chagas Filho - C.C.S., Laboratório de Fisiologia da Respiração Ilha do Fundão, 21949-900 - Rio de Janeiro, Brazil.
Fax: 55 2122808193
E-mail: wazin@biof.ufrj.br

Keywords: Inflammation, lung morphometry, phosphodiesterase inhibitor, respiratory mechanics

Received: November 26 2002
Accepted after revision: March 16 2003

This study was supported by the Centres of Excellence Programme (PRONEX-MCT), Brazilian Council for Scientific and Technological Development (CNPq), Financing for Studies and Projects (FINEP) and Rio de Janeiro State Research Supporting Foundation (FAPERJ).

Acute respiratory distress syndrome (ARDS) remains a common cause of morbidity and mortality. Although progress has been made in treating ARDS, no suitable therapeutic option exists and treatment is largely supportive. Thus, the development of new drugs with an effective anti-inflammatory profile would be extremely valuable.

Lately, a strategy that has received much attention relates to the level of cyclic adenosine monophosphate (cAMP) and cyclic guanosine monophosphate (cGMP) in the cells participating in the inflammatory process. Cyclic nucleotide second messengers (cAMP and cGMP) play a central role in signal transduction and regulation of physiological responses. Their intracellular levels are controlled by the superfamily of cyclic phosphodiesterase (PDE) enzymes. Inhibition of PDE family members increases intracellular cAMP and cGMP levels, thus exhibiting significant anti-inflammatory and disease-modifying effects, associated with the suppression of immune and inflammatory cells [1].

It is well documented that elevated levels of cAMP, mediated predominantly through inhibition of PDE4, suppress tumour necrosis factor (TNF)-α production and modulate the activity of virtually all cells involved in the inflammatory process [1–6]. Rolipram, a potent PDE4 inhibitor, effectively inhibits acute lung injury (ALI) induced by *Escherichia coli* lipopolysaccharide (LPS) when administered before or after LPS [5]. Its protective effect is associated with reduced pro-inflammatory cytokine production, inhibition of neutrophil accumulation in the lungs [1–5] and attenuated polymorphonuclear activation after sequestration [5]. Selective PDE5 inhibitors (sildenafil and zaprinast) block the hydrolysis of cGMP with minimal effects on the metabolism of cAMP [7–10]. Therefore, these PDE inhibitors not only augment the effect of combined inhaled nitric oxide [7–10], but produce selective pulmonary vasodilatation without a systemic counterpart when given alone [8–10]. Thus, pulmonary vascular resistance and capillary pressure would decrease, promoting the resolution of pulmonary oedema and improving gas exchange.

Presently, the clinical efficacy of the available PDE inhibitors on ARDS remains uncertain. Pentoxifylline, a non-selective PDE inhibitor, may have clinical potential in the treatment of ARDS [11–13], but there is not enough information to allow definite recommendations for clinical use. In addition, a recent trial by the National Institutes of Health ARDS Network showed no beneficial effects of lisofylline therapy in established ALI/ARDS [14]. Lisofylline is a compound chemically related to pentoxifylline, but its mechanism of action is unrelated to PDE effects [15].

LASSBio596 [16], designed as a hybrid of thalidomide and sildenafil, is a new agent that exhibits potent inhibitory effects

on PDE types 4 and 5, which are the main isozymes distributed in the lungs [1]. The current study was undertaken to test the effects of LASSBio596 when administered either prior to or after the induction of *E. coli* LPS ALI on *in vivo* and *in vitro* respiratory mechanics, and to correlate these results with collagen fibre content, bronchoalveolar lavage fluid (BALF) and lung morphometric analysis.

Materials and methods

Animal preparation

Twenty-four BALB/c mice (20–25 g) were randomly divided into four groups (n=6). In the control group, saline (0.05 mL) was instilled intratracheally (*i.t.*). The LPS group received LPS (*E. coli* O55:B5, 10 μg in 0.05 mL of saline per mouse *i.t.*). For intratracheal instillation, mice were treated with sevoflurane anaesthesia, a 1-cm midline cervical incision was made to expose the trachea, and then LPS or saline was instilled with a bent 27-gauge needle mounted on a tuberculin syringe. The cervical incision was closed with 5.0 silk suture and the mice were returned to their cage. The animals recovered rapidly after surgery. In the LASSBio596 groups, animals were treated with LASSBio596 (10 mg·kg body weight^{-1}, 0.2 mL) intraperitoneally (*i.p.*), 1 h before or 6 h after LPS administration.

LASSBio596 was structurally designed as a hybrid of thalidomide and the PDE inhibitor sildenafil [16]. Hydrolysis of the phthalimide framework was performed to remove the teratogenic effects of thalidomide [16].

Twenty-four hours later, the animals were sedated with diazepam (1 mg *i.p.*), anaesthetised (pentobarbital sodium, 20 mg·kg body weight^{-1} *i.p.*) and a snugly fitting cannula (0.8 mm internal diameter (ID)) was introduced into the trachea. Mechanical ventilation (model 683; Harvard Apparatus, Southnatick, MA, USA), with a frequency of 100 breaths·min^{-1}, a tidal volume (VT) of 7 mL·kg^{-1} and positive end-expiratory pressure of 2.0 cmH_2O, was applied. The anterior chest wall was surgically removed.

A pneumotachograph (1.5 mm ID, length 4.2 cm, distance between side ports 2.1 cm) was connected to the tracheal cannula for the measurements of airflow and changes in lung volume [17]. The pressure gradient across the pneumotachograph was determined by means of a Validyne MP45-2 differential pressure transducer (Engineering Corp., Northridge, CA, USA). The flow resistance of the equipment, tracheal cannula included, was constant up to flow rates of 26 mL·s^{-1} and amounted to 0.12 cmH_2O·mL^{-1}·s^{-1}. Equipment resistive pressure was subtracted from pulmonary resistive pressure, so that the present results represent intrinsic values. Tracheal pressure was measured with a Validyne MP-45 differential pressure transducer (Engineering Corp.). All signals were conditioned and amplified in a Beckman type R Dynograph (Beckman, Schiller Park, IL, USA). Flow and pressure signals were also passed through eight-pole Bessel filters (902LPF; Frequency Devices, Haverhill, MA, USA), with the corner frequency set at 100 Hz, sampled at 200 Hz with a 12-bit analogue-to-digital converter (DT2801A; Data Translation, Marlboro, MA, USA), and stored on a microcomputer. All data were collected using LABDAT software (RHT-Info Data Inc., Montreal, QU, Canada).

Measurement of pulmonary mechanics

Muscle relaxation was achieved with gallamine triethyliodide (2 mg·kg body weight^{-1} *i.v.*) and a constant flow ventilator provided artificial ventilation (Samay VR15; Universidad de la Republica, Montevideo, Uruguay). Special care was taken to keep VT (0.2 mL) and flow (1 mL·s^{-1}) constant in all animals in order to avoid the effects of different flows, volumes and inspiratory duration on the measured variables.

Pulmonary mechanics were measured by the end-inflation occlusion method [18, 19]. In an open chest preparation, tracheal pressure reflects transpulmonary pressure [20]. Pulmonary resistive, viscoelastic/inhomogeneous and total pressures, static elastance and dynamic elastance, and the difference between dynamic and static elastances were determined. Pulmonary mechanics measurements were performed 10 times in each animal. Data are presented as mean±SEM for each group.

Measurement of tissue mechanics

Heparine (1,000 IU) was intravenously injected immediately after the determination of respiratory mechanics. The trachea was clamped 10 min later at end-expiration, and the abdominal aorta and vena cava were sectioned, yielding a massive haemorrhage that quickly killed the animals. The lungs were removed *en bloc*, and placed in a modified Krebs-Henseleith (K-H) solution containing (mM) 118.4 NaCl, 4.7 KCl, 1.2 K_3PO_4, 25 $NaHCO_3$, 2.5 $CaCl_2 \cdot H_2O$, 0.6 $MgSO_4 \cdot H_2O$ and 11.1 glucose; at pH 7.40 and at 6°C. A 2×2×10-mm strip of subpleural parenchyma was cut from the periphery of each left lung and suspended vertically in an organ bath filled with K-H solution maintained at 37°C, continuously bubbled with a mixture of 95% oxygen and 5% carbon dioxide.

Lung strips were weighed and their unloaded resting lengths were determined with a calliper. Lung strip volume (V) was measured by simple densitometry, as follows:

$$V = \Delta F / \delta \quad (1)$$

where ΔF is the total change in force before and after strip immersion in K-H solution and δ is the mass density of the K-H solution [21–23].

One end of the material was attached to a force transducer (FT03; Grass Instruments Co., Quincy, MA, USA), while the other end was fastened to a vertical rod. This fibreglass stick was connected to the cone of a woofer, which was driven by the amplified sinusoidal signal of a waveform generator (3312A Function Generator; Hewlett Packard, Beaverton, OR, USA). A side arm of the rod was linked to a second force transducer by means of a silver spring of known Young′s modulus, thus allowing the measurement of displacement. Length and force output signals were conditioned (Gould 5900 Signal Conditioner Frame; Gould Inc., Valley View, OH, USA), fed through eight-pole Bessel filters (902LPF; Frequency Devices), analogue-to-digital converted (DT2801A; Data Translation Inc.) and stored on a computer. All data were collected using LABDAT software (RHT-InfoData Inc.). The frequency response of the system was dynamically studied by using calibrated silver springs with different elastic Young′s modulus. Neither amplitude dependence (<0.1% change in stiffness) nor phase changes with frequency were detected in the range of 0.01–14 Hz. The hysteresivity of the system was independent of frequency and had a value <0.003 [22, 23].

Each parenchymal strip was preconditioned by sinusoidal oscillation of the tissue during 30 min (frequency 1 Hz; amplitude large enough to reach a maximal stress of 20 g·cm^{-2}). Thereafter, the amplitude was adjusted to 5% of the unloading resting length and the oscillation was maintained for another 30 min or until a stable length/force loop

was reached. The isometric stress adaptation period resulted in a final force of 0.5 g. After preconditioning, the strips were oscillated at a frequency of 1 Hz [22, 23].

Tissue resistance, elastance and hysteresivity were calculated from the oscillatory recordings according to FREDBERG and STAMENOVIC [24].

Lung morphometric analysis

Morphometric analysis was performed in excised lungs at functional residual capacity. Immediately after the removal of the lungs *en bloc*, the right lung was quick-frozen by immersion in liquid nitrogen and fixed with Carnoy′s solution [25]. After fixation, the tissue was embedded in paraffin. Blocks were cut to a thickness of 4 μm by a microtome. The slices were stained with haematoxylin-eosin. Two investigators, who were unaware of the origin of the material, performed the microscopic examination.

Morphometric analysis was performed with an integrating eyepiece with a coherent system made of a 100-point grid consisting of 50 lines of known length, coupled to a conventional light microscope (Axioplan; Zeiss, Oberkochen, Germany). Volume fractions of collapsed and normal pulmonary areas were determined by the point-counting technique, made across 10 random noncoincident microscopic fields at a magnification of ×400 [26]. Lung tissue distortion was assessed by measuring the mean linear intercept between alveolar walls at a magnification of ×100 [26]. The mean linear intercept between alveolar walls was determined by counting the number of intercepts between the eyepiece lines and the alveolar septum of each microscopic field, and was expressed as the relation between the line length (1,250 μm) and the total number of intercepts. The internal diameter of the central airways was computed by counting the points falling on the airway lumen and those falling on airway smooth muscle and epithelium. The perimeter of the airways was estimated by counting the intercepts of the lines of the integrating eyepiece with the epithelial basal membrane. This procedure was repeated four times for each airway. The areas of smooth muscle and airway epithelium were corrected in terms of airway perimeter by dividing their values by the number of intercepts of the line system with the epithelial basal membrane of the corresponding airway. Since the number of intercepts (NI) of the lines with the epithelial basal membrane is proportional to airway perimeter, and the number of points (NP) falling on the airway lumen is proportional to airway area, the magnitude of bronchoconstriction (contraction index (CI)) was computed by the following relationship [27]:

$$CI = NI/\sqrt{NP} \quad (2)$$

Polymorphonuclear and mononuclear cells, and pulmonary tissue were evaluated at ×1,000 magnification. Points falling on tissue area were counted and divided by the total number of points in each microscopic field. Thus, data were reported as the fractional area of pulmonary tissue [26]. The same method was applied to determine polymorphonuclear and mononuclear cells. The inflammation index was estimated by the relationship between the number of polymorphonuclear cells and the number of intersections of the alveolar septa.

Morphometric analysis of the parenchymal strips

At the end of the experiments, the organ bath was removed and the parenchymal strips were frozen by rapid immersion in liquid nitrogen at the force maintained during the experiment. Frozen strips were fixed as aforementioned. Sections were examined at ×400 magnification, and the fractional areas of alveolar wall, blood-vessel wall and bronchial wall were determined by the point-counting technique [26]. This analysis was performed in 10 random nonoverlapping fields in each strip.

The tissue slices also underwent the picrosirius polarisation method to characterise the collagenous fibre system in the alveolar septa [28]. Quantification was carried out with the aid of a digital analysis system and specific software (Bioscan-Optimas 5:1; Bioscan Inc., Edmond, WA, USA) under ×200 magnification. The images were generated by a microscope (Axioplan; Zeiss) connected to a camera (Sony Trinitron CCD; Sony, Tokyo, Japan), fed into a computer through a frame grabber (Oculus TCX; Coreco Inc., St Laurent, PQ, Canada) for offline processing. The thresholds for fibres of the collagenous system were established after enhancing the contrast up to a point at which the fibres were easily identified as birefringent (collagen) bands. The area occupied by fibres was determined by digital densitometric recognition. Bronchi and blood vessels were carefully avoided during the measurements. The areas occupied by the collagen fibres were divided by the length of each studied septum, in order to avoid any bias due to septal oedema or alveolar collapse. The results were expressed as the amount of collagen fibres per unit of septal length.

Evaluation of bronchoalveolar lavage fluid

Another eight to 16 animals of each group were submitted to the aforementioned protocol in order to obtain aliquots of BALF. For this purpose, 24 h after saline or LPS instillation, the animals were anaesthetised (pentobarbital sodium, 12 mg·kg body weight^{-1} *i.p.*), the trachea was cannulated and the lungs washed eight times with 0.5 mL of saline to provide 4 mL of BALF. Aliquots of each BALF were used to evaluate total and differential cell numbers and TNF-α level.

Total cells present in the BALF were counted with a Coulter counter ZM (Coulter Electronics, Hialeah, FL, USA) and values were expressed as number of cells·mL^{-1}. Differential cell counts were performed after cytocentrifugation (Shandon, East Grinstead, UK) and staining with Diff-Quick stain (Baxter Dade AG, Dunding, Germany). At least 250 cells were counted and the results were expressed as number of cell population·mL^{-1} [29, 30].

After centrifugation of the BALF, the supernatant was collected and stored at -70°C. The supernatant was then assayed for TNF-α levels. TNF-α levels in the BALF were determined by a highly specific enzyme-linked immunosorbent assay with a detection limit of 50 pg·mL^{-1} [29, 30].

Statistical analysis

The mechanical, morphometrical and BALF parameters gathered from the control, LPS, LASSBio596 before and after groups were compared using a one-way analysis of variance. If multiple comparisons were then required, the Student-Newman-Keuls test was applied. The relationships between mechanical and morphometrical parameters were evaluated by Spearman correlation. In all tests the significance level was set at 5%.

Results

There was no statistically significant difference in flow and volume among the groups. Dynamic and static elastances,

total, resistive and viscoelastic/inhomogeneous pressures, tissue elastance and resistance, and hysteresivity were all higher in the LPS group compared with the other groups (table 1).

Histological changes in the LPS group included interstitial and alveolar oedema, atelectasis, inflammation with polymorphonuclear cells, hyaline membrane, airway infiltration of neutrophils and inflammatory oedema; features that all contribute to a reduced airway calibre. These changes were not observed when LASSBio596 was administered 1 h before or 6 h after LPS-induced ALI (fig. 1).

The mean±SEM percentages of normal and collapsed areas,

Table 1. – *In vivo* and *in vitro* mechanical parameters

	Control	LPS	596-b	596-a
In vivo				
V' $mL \cdot s^{-1}$	1.03±0.01	1.01±0.01	1.01±0.01	1.01±0.01
V $mL \cdot s^{-1}$	0.21±0.01	0.21±0.01	0.20±0.01	0.20±0.01
Est $cmH_2O \cdot mL^{-1}$	26.27±1.21	43.25±3.20*	23.96±1.33	24.60±1.33
Edyn $cmH_2O \cdot mL^{-1}$	29.88±1.23	47.94±3.33*	27.82±1.37	28.31±1.36
ΔE $cmH_2O \cdot mL^{-1}$	3.61±0.16	4.70±0.18*	3.86±0.17	3.71±0.13
ΔPtot cmH_2O	1.21±0.04	1.60±0.06*	1.21±0.04	1.17±0.03
$\Delta P1$ cmH_2O	0.47±0.02	0.63±0.03*	0.46±0.01	0.41±0.01
$\Delta P2$ cmH_2O	0.74±0.04	0.97±0.04*	0.75±0.03	0.75±0.02
In vitro				
E $N \cdot m^{-2} \cdot 10^{-4}$	0.98±0.04	1.46±0.04*	1.17±0.06	1.06±0.07
R $N \cdot s^{-1} \cdot m^{-2} \cdot 10^{-2}$	1.05±0.02	1.57±0.07*	1.10±0.09	1.15±0.07
η	0.07±0.01	0.08±0.01*	0.07±0.01	0.07±0.01

Data are presented as means±SEM of six animals (10 determinations per mouse). Data are shown for control, lipopolysaccharide (LPS), LASSBio596 1 h before LPS (596-b) and LASSBio596 6 h after LPS (596-a) groups. V': gas flow; V: volume; Est: pulmonary static elastance; Edyn: pulmonary dynamic elastance; ΔE: difference between dynamic and static elastances; ΔPtot: total pressure; $\Delta P1$: resistive pressure; $\Delta P2$: viscoelastic/inhomogeneous pressure; E: tissue elastance; R: resistance; η: hysteresivity. *: $p<0.05$ *versus* the other groups.

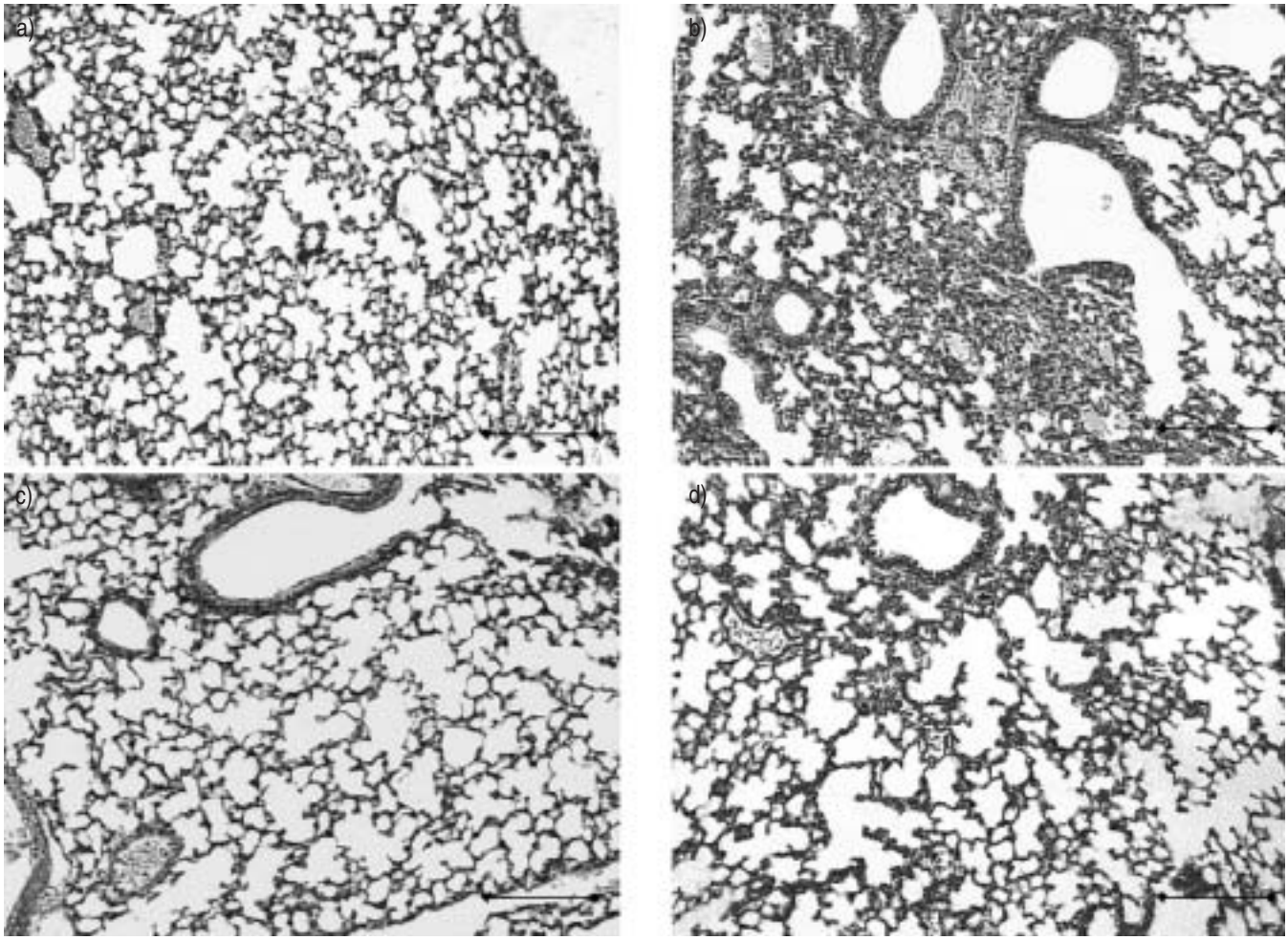

Fig. 1. – Photomicrographs of lung parenchyma stained with haematoxylin-eosin: a) control, b) acute lung injury (ALI) induced by *Escherichia coli* lipopolysaccharide, c) treatment with LASSBio596 1 h before or d) 6 h after ALI induction. Scale bars=100 μm.

Table 2. – Morphometrical parameters

Groups	Normal area %	Alveolar collapse %	Inflammation index	Lm μm	Contraction index
Control	99.2±0.2	0.8±0.1	0.2±0.01	59.5±1.6	1.73±0.03
LPS	19.3±2.4*	80.7±2.4*	0.6±0.02*	48.2±2.4*	2.06±0.03*
596-b	85.2±1.5*,#	14.8±1.5*,#	0.3±0.01*,#	61.3±0.6	1.85±0.04
596-a	74.9±0.5*,#,¶	25.1±0.5*,#,¶	0.3±0.01*,#	59.5±1.0	1.84±0.02

Data are presented as mean±SEM of six animals in each group (10 random, noncoincident fields per mouse). Data are shown for control, lipopolysaccharide (LPS), LASSBio596 1 h before LPS (596-b) and LASSBio596 6 h after LPS (596-a) groups. Lm: mean linear intercept between alveolar walls. *: p<0.05 *versus* control group; #: p<0.05 *versus* LPS group; ¶: p<0.05 *versus* 596-b.

mean linear intercept between alveolar walls, inflammation index and contraction index in the control, LPS, LASSBio596 before and after groups are listed in table 2. The fraction of alveolar collapse was higher in LPS than in the control group; although LASSBio596 lessened collapse in relation to LPS, the values were still higher than in control. LASSBio596 administered prior to ALI induction seemed to be more efficient in avoiding alveolar collapse. The LPS group presented smaller mean linear intercept between alveolar walls and central airway diameters (larger contraction index) than those found in the other groups (table 2). Total and polymorphonuclear cell contents were higher in the LPS group than in control, LASSBio596 before and after groups (table 3). These data suggest that LASSBio596 presents potent anti-inflammatory effects on ALI induced by *E. coli* LPS. Tissue strip morphometric analysis showed similar anatomic composition in all groups (table 4).

Collagen fibre content was greater in LPS (0.041±0.002 $\mu m^2 \cdot \mu m^{-1}$) than in the control group (0.012±0.003 $\mu m^2 \cdot \mu m^{-1}$) and LASSBio596 avoided the increment in the collagen fibre content independently of the time of injection (after: 0.012± 0.002 $\mu m^2 \cdot \mu m^{-1}$; before: 0.014±0.002 $\mu m^2 \cdot \mu m^{-1}$).

There was an increase in neutrophil numbers and an increment in TNF-α levels in the BALF 24 h after the *E. coli* LPS-induced ALI. LASSBio596, injected 1 h before or 6 h after LPS administration, prevented increases in the neutrophil content and TNF-α levels in the BALF (fig. 2).

Table 3. – Cellularity in lung parenchyma

Groups	Total %	PMN %	MN %
Control	20.7±0.80	15.5±1.06	5.2±0.36
LPS	31.3±1.87*	27.8±2.46*	3.5±0.98
596-b	23.9±1.44	20.9±1.72	3.0±1.10
596-a	20.4±0.42	16.8±1.73	5.2±0.75

Data are presented as mean±SEM of six lungs in each group (10 microscopic fields were analysed in each lung). Data are shown for control, lipopolysaccharide (LPS), LASSBio596 1 h before LPS (596-b), and LASSBio596 6 h after LPS (596-a) groups. Total: total cellular fractional area; PMN: polymorphonuclear cell fractional area; MN: mononuclear cell fractional area. *: p<0.05 *versus* the other groups.

Table 4. – Volume proportions of alveolar (AW), blood vessel (BVW) and bronchial (BW) walls in parenchymal strips

Groups	AW %	BVW %	BW %
Control	92.2±0.2	4.7±0.2	3.2±0.1
LPS	92.4±0.1	4.3±0.1	3.4±0.2
596-b	92.2±0.3	4.6±0.3	3.2±0.2
596-a	92.3±0.3	4.6±0.2	3.1±0.2

Data are presented as mean±SEM of six strips in each group (10 microscopic fields were analysed in each strip). Data are shown for control, lipopolysaccharide (LPS), LASSBio596 1 h before LPS (596-b) and LASSBio596 6 h after LPS (596-a) groups.

Considering the control, LPS, LASSBio596 before and after groups together, static elastance and viscoelastic/inhomogeneous pressures were well correlated with the fraction of area of alveolar collapse, the inflammation index and the mean linear intercept between alveolar walls, as shown in table 5. Resistive pressure was correlated with the contraction index. Tissue elastance and resistance, and hysteresivity were related to total cell count (p=0.004, p= 0.01 and p=0.01, respectively), and with polymorphonuclear cell count (p=0.003, p=0.011 and p=0.005, respectively). Hysteresivity was correlated with collagen fibre content (p=0.014).

Discussion

This study demonstrated that treatment with LASSBio596 can avoid increases in *in vivo* and *in vitro* pulmonary impedance caused by LPS administration, when given either 1 h prior to or 6 h after ALI induction. LASSBio596 also modulated the lung inflammatory process elicited by LPS.

A model of LPS-induced ALI was applied to mimic the morphological and functional changes observed in clinical situations resulting from circulating LPS. It is well documented that LPS administration triggers a network of inflammatory responses mediated by a number of immune cells, which is followed by the release of a vast array of pro-inflammatory mediators that orchestrate the acute inflammatory response [29, 30]. LPS promotes activation of mononuclear phagocytes, leading to the release of different cytokines, including TNF-α, which induces neutrophil adherence to endothelial cells, and facilitates migration and infiltration of polymorphonuclear cells into pulmonary spaces. Neutrophil activation

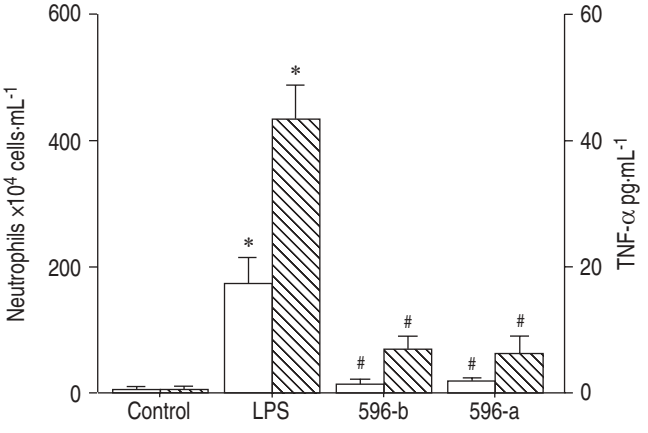

Fig. 2. – Neutrophil (□) and tumour necrosis factor (TNF)-α (▨) recruitment in bronchoalveolar lavage fluid in control, lipopolysaccharide (LPS), LASSBio596 1 h before LPS (596-b) and 6 h after LPS (596-a) groups. Data are presented as mean±SEM. *: p<0.05 *versus* control group; #: p<0.05 *versus* LPS group.

Table 5. – Correlation matrix between physiological and morphometric parameters

	Contraction index	Collapse %	Inflammation index	Lm μm
E_{st} $cmH_2O \cdot mL^{-1}$	0.42 (0.044)	0.44 (0.029)	0.42 (0.041)	-0.47 (0.021)
$\Delta P2$ cmH_2O	0.46 (0.023)	0.52 (0.009)	0.64 (0.001)	-0.60 (0.002)
$\Delta P1$ cmH_2O	0.42 (0.041)	0.38 (NS)	0.46 (0.024)	-0.60 (0.002)

The correlation was performed on data from control, lipopolysaccharide (LPS), LASSBio596 1 h before LPS and 6 h after LPS groups. All p-values are shown in brackets. Lm: mean linear intercept between alveolar walls; E_{st}: pulmonary static elastance; $\Delta P2$: viscoelastic/inhomogeneous pressure; $\Delta P1$: resistive pressure; NS: nonsignificant.

produces oxygen radicals and releases granular enzymes that are associated with the development of ALI [30]. The intratracheal instillation of LPS induced *in vivo* and *in vitro* respiratory mechanical changes (table 1) associated with lung morphometrical alterations, an increment in TNF-α levels, collagen fibre deposition in the alveolar septa and neutrophil infiltration in the lung tissue and BALF (table 2, figs 1 and 2).

LASSBio596, structurally designed as a hybrid of thalidomide and the PDE inhibitor sildenafil, exhibited important anti-inflammatory and immunomodulatory profiles [16]. The molecule of this new thalidomide analogue lacks the phthalimide ring (responsible for the teratogenic effects of thalidomide), thus, possibly avoiding an eventual teratogenic effect. LASSBio596 modulates the inflammatory process by inhibiting PDE4 and 5, which regulate the breakdown of the intracellular second messengers cAMP and cGMP, respectively [16].

The administration of LASSBio596 1 h before or 6 h after LPS instillation inhibited alterations in *in vivo* mechanical parameters (table 1). Interestingly, respiratory mechanics and histological lung changes observed at 24 h were already present as early as 6 h after ALI induction, although less intense. ASTI *et al.* [31] also observed a massive margination of polymorphonuclear cells in lung parenchyma and in the BALF with a similar dose of intratracheal LPS. They demonstrated a significant increase in lung myeloperoxidase activity at 4 h (131% increase *versus* controls, $p<0.001$) and 6 h (147% increase *versus* controls, $p<0.001$). Thus, LASSBio596 was given both when lung dysfunction was present and after the inflammatory cascade was initiated.

LASSBio596 attenuated the increases in BALF TNF-α levels (fig. 2) and inhibited pulmonary neutrophilia (table 3). The precise mechanism whereby LASSBio596 attenuates lung inflammation is not known. In accordance with the literature, PDE4 and 5 inhibitors may lead to the suppression of chemoattractant and pro-inflammatory cytokine release [2–5, 29], the downregulation of cell adhesion molecules [1], the inhibition of leukocyte migration [2, 5], functional inhibition of the various types of cells including lung macrophages, neutrophils, lymphocytes, and monocytes [1, 2, 5, 32], and increased macrophage anti-inflammatory cytokine production [32].

LASSBio596 is a potent anti-inflammatory agent and it could be expected to increase susceptibility to infection. Of the animals, 40% died of diffuse lung oedema at day 1 after intratracheal instillation of LPS alone, whilst the animals that received LASSBio596 presented a significantly higher survival rate (100%) at day 1 ($p<0.001$), which remained unchanged until 4 weeks after ALI induction. At 4 weeks, the macroscopic aspects of the lungs from animals treated with LASSBio596 were similar to those of the control group. Immediately after ALI induction, the animals were housed for 4 weeks in conventional open cages and with access to standard food and water *ad libitum*. Thus, the environmental conditions associated with the inhibition of neutrophilia and the TNF-α production did not induce infection nor the increased mortality rate

LASSBio596 anti-inflammatory effects in LPS-induced ALI were similar to those observed with rolipram, the prototypic PDE4 inhibitor [2, 3, 30]. In addition, in a model of ALI induced by LPS followed by zymozan, rolipram inhibited lung injury when given before or after LPS through the attenuation of neutrophil activation even after sequestration, apparently independently of TNF-α inhibition [5].

LASSBio596 also prevented the reduction of central airway calibre (table 2). PDE4 inhibition could explain this phenomenon by airway smooth muscle relaxation, modulation of the activity of pulmonary nerves and suppression of the activation of inflammatory cells, thus modulating the bronchomotor tone [1, 33]. Additionally, LASSBio596 attenuated the alveolar collapse observed in the LPS group, suggesting that it might diminish the impairment of the surfactant system usually observed in injured lungs. HAFNER and GERMANN [34] demonstrated that combined treatment with protein-C-based surfactant, rSP-C, and a PDE4 inhibitor, roflumilast, led to improved oxygenation and inhibition of hyaline membrane formation in a lung lavage model of ALI. This information supports the current histopathological findings presented in LASSBio596 before and after groups, which did not demonstrate hyaline membrane formation.

The method used to determine tissue mechanical properties in this study avoids the effects of surface film, alveolar flooding and airway inhomogeneity. Thus, a direct analysis of the role of fibre-to-fibre networking within the connective tissue matrix on tissue mechanical properties is ensured [22–24, 35]. The current study is the first analysis of tissue mechanical properties by oscillation of lung parenchymal strips in an *E. coli* LPS model of ALI. Elastance, resistance and hysteresivity of LPS-treated mice were significantly increased in comparison with control tissue, suggesting that parenchymal mechanical dysfunction plays an important role in the pathophysiology of ALI (table 1). These modifications happened in an early phase of the lesion, and were accompanied by cellular polymorphonuclear infiltration in lung parenchyma and deposition of collagen fibres. The present results show that the collagen content was already elevated 24 h after tissue damage with *E. coli* LPS, indicating that the biochemical processes implicated in collagen synthesis are indeed able to react very quickly. LASSBio596 avoided tissue mechanical changes in LPS-induced ALI (table 1) by inhibiting collagen fibre deposition in the alveolar septa and preventing polymorphonuclear infiltration into the lung parenchyma. The modulating effect of LASSBio596 on the connective matrix remodelling is in line with previous reports [36–38], showing that PDE4 inhibitors are able to suppress fibroblast activity, and, thus, have the potential to block the development of progressive fibrosis.

Oedema formation was observed in the present model of ALI. LASSBio596, however, demonstrated a protective effect against pulmonary oedema formation, possibly by: 1) the anti-inflammatory effects of PDE4 inhibition, as described previously [1–6, 30, 32]; and 2) pulmonary vasodilatation *via* the inhibition of cGMP inactivation by PDE5 [7–10].

Pentoxifylline, a nonselective PDE inhibitor, has been used

to treat septic patients, as it improves cardiopulmonary function and reduces the mortality rate [12, 13]. Additionally, CREAMER *et al.* [39] showed that pentoxifylline, given as a rescue agent, prevents deterioration of lung compliance and preserves vascular integrity. Therefore, experimental studies and limited clinical experience in humans suggest that pentoxifylline may have a clinical potential in the treatment of ARDS. Conversely, lisofylline has no beneficial effects in the treatment of established ALI/ARDS [14]. Lisofylline is a new compound chemically related to pentoxifylline with potential biological activity unrelated to PDE effects. It inhibits the generation of phosphatidic-acid species, which act as intermediary messengers with selective pro-inflammatory targets [15]. New PDE inhibitors with more selective targets are under development for clinical use and may have significant clinical potential in the treatment of ARDS.

To conclude, LASSBio596 effectively prevented respiratory and tissue mechanical changes, minimised lung morphometrical alterations and had the potential to block lung fibroproliferation in a mouse model of *Escherichia coli* lipopolysaccharide-induced acute lung injury. Thus, LASSBio596 displayed an important anti-inflammatory profile and may act on the pulmonary vasculature, suggesting that the use of agents that inhibit phosphodiesterase 4 and 5 simultaneously could be a useful adjunct therapy for acute lung injury. Mouse and man clearly share many basic physiological processes; nonetheless each animal model should be viewed as one component of the process for studying human disease and not viewed in isolation nor extrapolated directly to humans.

Acknowledgements. The authors would like to express their gratitude to E.M. Negri for comments and advice, to F.O. Leal for help in morphometric analysis and to A. Carlos de Souza Quaresma and R. da Conceição Pereira Milho for their skilful technical assistance.

References

1. Essayan DM. Cyclic nucleotide phosphodiesterases. *J Allergy Clin Immunol* 2001; 108: 671–680.
2. Sekut L, Yarnall D, Stimpson SA, *et al.* Anti-inflammatory activity of phosphodiesterase (PDE)-IV inhibitors in acute and chronic models of inflammation. *Clin Exp Immunol* 1995; 100: 126–132.
3. Turner CR. Therapeutic intervention in a rat model of ARDS: IV. Phosphodiesterase IV inhibition. *Circ Shock* 1993; 39: 237–245.
4. Spond J, Chapman R, Fine J, *et al.* Comparison of PDE 4 inhibitors, Rolipram and SB 207499 (Ariflo^{TM}), in a rat model of pulmonary neutrophilia. *Pulm Pharmacol Ther* 2001; 14: 157–164.
5. Miotla JM, Teixeira MM, Hellewell PG. Suppression of acute lung injury in mice by an inhibitor of phosphodiesterase type 4. *Am J Respir Cell Mol Biol* 1998; 18: 411–420.
6. Howell RE, Jenkins LP, Howell DE. Inhibition of lipopolysaccharide-induced pulmonary edema by isozyme-selective phosphodiesterase inhibitors in guinea pig. *J Pharmacol Exp Ther* 1995; 275: 703–709.
7. Steinhorn RH, Gordon JB, Tod ML. Site-specific effect of guanosine 3′,5′-cyclic monophosphate phosphodiesterase inhibition in isolated lamb lungs. *Crit Care Med* 2000; 28: 490–495.
8. Holzmann A, Manktelow C, Weimann J, Bloch KD, Zapol WM. Inhibition of lung phosphodiesterase improves responsiveness to inhaled nitric oxide in isolated-perfused lungs from rats challenged with endotoxin. *Intensive Care Med* 2001; 27: 251–257.
9. Ichinose F, Adrie C, Hurford W, Bloch K, Zapol W. Selective pulmonary vasodilation induced by aerosolized Zaprinast. *Anesthesiology* 1998; 88: 410–416.
10. Ichinose F, Erana-Garcia J, Hromi J, *et al.* Nebulized sildenafil is a selective pulmonary vasodilator in lambs with acute pulmonary hypertension. *Crit Care Med* 2001; 29: 1000–1005.
11. Zabel P, Schonharting MM, Wolter DT, Schade UF. Oxpentifylline in endotoxaemia. *Lancet* 1989; 2: 1474–1477.
12. Staubach KH. Effect of pentoxifylline in severe sepsis: results of a randomized, double-blind, placebo-controlled study. *Arch Surg* 1998; 133: 94–100.
13. Lauterbach R. Effect of the immunomodulating agent, pentoxifylline, in the treatment of sepsis in prematurely delivered infants: a placebo-controlled, double-blind trial. *Crit Care Med* 1999; 27: 807–814.
14. The ARDS Clinical Trials Network. Randomized, placebo-controlled trial of lisofylline for early treatment of acute lung injury and respiratory distress syndrome. *Crit Care Med* 2002; 30: 1–6.
15. Rice GC, Brown PA, Nelson RJ, Bianco JA, Singer JW, Bursten S. Protection from endotoxic shock in mice by a pharmacologic inhibition of phosphatidic acid. *Proc Natl Acad Sci USA* 1994; 91: 3857–3861.
16. Lima ML, Castro P, Machado AL, *et al.* Synthesis and anti-inflammatory activity of phthalimide derivatives, designed as new thalidomide analogues. *Bioorg Med Chem* 2002; 10: 3067–3073.
17. Mortola JP, Novoraj A. Two-sidearm tracheal cannula for respiratory airflow measurements in small animals. *J Appl Physiol* 1983; 55: 250–253.
18. Bates JHT, Baconnier P, Milic-Emili J. A theoretical analysis of the interrupter technique for measuring respiratory mechanics. *J Appl Physiol* 1988; 64: 2204–2214.
19. Similowski T, Levy P, Corbeil C, *et al.* Viscoelastic behavior of lung and chest wall in dogs determined by flow interruption. *J Appl Physiol* 1989; 67: 2219–2229.
20. Agostoni E, Mead J. Statics of the respiratory system. *In*: Fenn WO, Rahn H, eds. Handbook of Physiology. Respiration. Washington, American Physiological Society, 1964; pp. 387–409.
21. Lopez-Aguilar J, Romero PV. Effect of elastase pretreatment on rat lung strip induced constriction. *Respir Physiol* 1998; 113: 239–246.
22. Rocco PRM, Negri EM, Kurtz PM, *et al.* Lung tissue mechanics and extracellular matrix remodelling in acute lung injury. *Am J Respir Crit Care Med* 2001; 164: 1067–1071.
23. Faffe DS, Silva GH, Kurtz PMP, *et al.* Lung tissue mechanics and extracellular matrix composition in a murine model of silicosis. *J Appl Physiol* 2001; 90: 1400–1406.
24. Fredberg JJ, Stamenovic D. On the imperfect elasticity of lung tissue. *J Appl Physiol* 1989; 67: 2408–2414.
25. Nagase T, Dallaire MJ, Ludwig MS. Airway and tissue behavior during early response in sensitized rats: role of 5-HT and LTD4. *J Appl Physiol* 1996; 80: 583–590.
26. Weibel ER. Morphometry: stereological theory and practical methods. *In*: Gil J, ed. Models of Lung Disease - Microscopy and Structural Methods. New York, Marcel Dekker, 1990; pp. 199–247.
27. Sakae RS, Leme AS, Dolnikoff M, *et al.* Neonatal capsaicin treatment decreases airway and pulmonary tissue responsiveness to methacholine. *Am J Physiol* 1994; 2669: 223–229.
28. Montes GS. Structural biology of the fibers of the collagenous and elastic system. *Cell Biol Int* 1996; 20: 15–27.
29. Faffe DS, Seidl VR, Chagas PSC, *et al.* Respiratory effects of lipopolysaccharide-induced inflammatory injury in mice. *Eur Respir J* 2000; 15: 85–91.
30. Gonçalves de Moraes VL, Singer M, Boris Vargaftig B, Chignard M. Effect of rolipram on cyclic AMP levels in alveolar macrophages and lipopolysaccharide-induced inflammation in mouse lung. *Br J Pharmacol* 1998; 123: 631–636.

31. Asti C, Puggieri V, Porzio S, Chiusaroli R, Melillo G, Caselli GF. Lipopolysaccharide-induced lung injury in mice. I. Concomitant evaluation of inflammatory cells and haemorrhagic lung damage. *Pulm Pharmacol Ther* 2000; 13: 61–69.
32. Kambayashi T, Jacob CO, Zhou D, Mazurek N, Fong M, Strassmann G. Cyclic nucleotide phosphodiesterase type IV participates in the regulation of IL-10 and in the subsequent inhibition of TNF-α and IL-6 release by endotoxin-stimulated macrophages. *J Immunol* 1995; 155: 4909–4916.
33. Toward TJ, Broadey KJ. Goblet cell hyperplasia, airway function, and leukocyte infiltration after chronic lipopolysaccharide exposure in conscious Guinea pigs: effects of rolipram and dexamethasone. *J Pharmacol Exp Ther* 2002; 302: 814–821.
34. Hafner D, Germann PG. Additive effects of phosphodiesterase-4 inhibition on effects of rSP-C surfactant. *Am J Respir Crit Care Med* 2000; 161: 1495–1500.
35. Yuan H, Ingenito EP, Suki B. Dynamic properties of lung parenchyma: mechanical contributions of fiber network and interstitial cells. *J Appl Physiol* 1997; 83: 1420–1431.
36. Kohyama T, Liu X, Zhu Y, Wen FQ, Wang H, Rennard SI. Phosphodiesterase inhibitor attenuation of fibroblast chemotaxis depends on endogenous prostaglandin production. *Chest* 2001; 120: 14S–15S.
37. Kohyama T, Liu X, Wen FQ, *et al.* PDE 4 inhibitors attenuate fibroblast chemotaxis and contraction of native collagen gels. *Am J Respir Cell Mol Biol* 2002; 26: 694–701.
38. Corbel M, Germain N, Lauchou J, *et al.* The selective phosphodiesterase 4 inhibitor RP 73-401 reduced matrix metalloproteinase 9 activity and transforming growth factor-β release during acute lung injury in mice: the role of the balance between tumor necrosis factor-α and interleukin-10. *J Pharmacol Exp Ther* 2002; 301: 258–265.
39. Creamer KM, McCloud LL, Fisher LE, Ehrhart IC. Pentoxifylline rescue preserves lung function in isolated canine lungs injured with phorbol myristate acetate. *Chest* 2001; 119: 1893–1900.